Strength formation mechanism and performance of steel slag self-compacting epoxy resin concrete

Li, Yuanyuan; Li, Jun; Li, Chao; Chen, Anqi; Bai, Tao; Tang, Shimin; Wu, Shaopeng; Gao, Yangming; Zhu, Hongbin; Feng, Jianlin

DOI
10.1016/j.conbuildmat.2022.129525

Publication date
2022

Document Version
Final published version

Published in
Construction and Building Materials

Citation (APA)
Li, Y., Li, J., Li, C., Chen, A., Bai, T., Tang, S., Wu, S., Gao, Y., Zhu, H., & Feng, J. (2022). Strength formation mechanism and performance of steel slag self-compacting epoxy resin concrete. *Construction and Building Materials*, *359*, Article 129525. https://doi.org/10.1016/j.conbuildmat.2022.129525

Construction and Building Materials 359 (2022) 129525

Contents lists available at ScienceDirect

Construction and Building Materials

journal homepage: www.elsevier.com/locate/conbuildmat

Strength formation mechanism and performance of steel slag self-compacting epoxy resin concrete

Yuanyuan Li [a], Jun Li [a], Chao Li [b], Anqi Chen [c,*], Tao Bai [a,*], Shimin Tang [a], Shaopeng Wu [c], Yangming Gao [d], Hongbin Zhu [a], Jianlin Feng [a]

[a] School of Civil Engineering and Architecture, Wuhan Institute of Technology, Wuhan 430074, China
[b] Foshan Transportation Science and Technology Co., Ltd, Foshan 528315, Guangdong, China
[c] State Key Laboratory of Silicate Materials for Architectures, Wuhan University of Technology, Wuhan 430070, Hubei, China
[d] Marie S. Curie Research Fellow Section of Pavement Engineering, Faculty of Civil Engineering & Geosciences, Delft University of Technology, Stevinweg 1, 2628 CN Delft, The Netherlands

ARTICLE INFO

Keywords:
Steel slag
Road expansion joints
Pavement repair
Micro morphology
Actual engineering verification

ABSTRACT

A self-compacting steel slag epoxy resin concrete (SERC) was designed with steel slag as aggregate and epoxy resin as binder for rapid repair of road expansion joints and pavement. At the same time, a group of self-compacting basalt epoxy resin concrete (BERC) with basalt as coarse aggregate and limestone as fine aggregate was set up as the control group. The element analysis and micro morphology of SERC and BERC were studied by X-ray fluorescence spectrometry (XRF) and scanning electron microscope (SEM) to reveal the strength-forming mechanism of the two epoxy resin concretes. The cube compression test and Marshall stability test were used to study the effect of the strength formation rate and temperature of SERC and BERC on the strength. In addition, the high-temperature stability, low-temperature crack resistance, water damage resistance, fatigue resistance and interlayer bonding properties of SERC and BERC were also studied. The results showed that both SERC and BERC have good mechanical properties, high temperature properties and good bonding properties, and the low-temperature crack resistance and fatigue properties of SERC are better than that of BERC. According to the verification of the actual project that has been in service for one year, SERC can be perfectly used for road expansion joints.

1. Introduction

Epoxy resin is a commonly used polymer material. Different from thermoplastic asphalt, epoxy resin road materials have good high-temperature resistance [1]. High-performance epoxy road materials also have excellent mechanical properties, corrosion resistance and fatigue resistance. Steel slag is a by-product of iron and steel manufacturing industry, with an annual output of about 360 million tons every year [2]. The output of steel slag is huge, but its properties are unstable and require pretreatment or long-term natural accumulation to stabilize its chemical properties [3]. Pretreatment of steel slag may reduce steel production or increase steelmaking costs [4]. The long-term natural accumulation of steel slag will not only waste land, but also pollute groundwater with heavy metals in steel slag [5]. Recycling steel slag as aggregate of concrete can reduce the consumption of natural aggregates, reduce the environmental harm caused by the accumulation of steel slag, and improve various service properties of pavement [6]. However, the high water absorption and self-expansion of steel slag [7] limit its large-scale application in asphalt concrete and cement concrete [8,9]. When epoxy resin is used as a binder to prepare epoxy resin concrete, it can effectively reduce the harmful effect of steel slag on epoxy resin concrete due to the high strength and toughness of epoxy resin after curing [10]. Therefore, epoxy resin concrete can be prepared with steel slag as the aggregate and epoxy resin as the binder.

In road and bridge engineering, a variety of materials are used for road and bridge expansion joints, road and bridge surface repair, and concrete structure crack reinforcement [11]. This kind of material generally requires good bonding, high strength, fast strength formation

* Corresponding authors.
E-mail addresses: Liyy@wit.edu.cn (Y. Li), 22104010113@stu.wit.edu.cn (J. Li), lic@whut.edu.cn (C. Li), anqi.chen@whut.edu.cn (A. Chen), baigs08@wit.edu.cn (T. Bai), 2001160618@stu.wit.edu.cn (S. Tang), wusp@whut.edu.cn (S. Wu), Y.Gao-3@tudelft.nl (Y. Gao), 22004010115@stu.wit.edu.cn (H. Zhu), 22004010110@stu.wit.edu.cn (J. Feng).

https://doi.org/10.1016/j.conbuildmat.2022.129525
Received 30 July 2022; Received in revised form 15 October 2022; Accepted 17 October 2022
Available online 26 October 2022

Table 1
Technical properties of A and B components of Epoxy resin binder.

Component	Raw materials	Density (g/cm^3)	25 °C Viscosity (CPS)	Test Methods
A Component	Epoxy resin	1.1	40000–45000	GB/T 2567-2008
B Component	Curing agent	1.2	45000–50000	GB/T 2567-2008

and good water tightness [12]. Compared with the main paving material, its dosage is very small, but it plays a great role in the durability and comfort of the road. According to the statistics at the end of the 20th century, more than half of the structural or functional defects or failures of roads and bridges occurred in expansion joints [13]. During the service of asphalt and cement pavement, various pits and cracks will appear due to various factors such as load, climate, light and so on [14]. Instead of replacing the whole damaged structure, it is better to find a material with high strength and fast strength formation as expansion joint material or repair material [15]. Portland cement concrete is a widely used material with certain serviceability, but its strength, toughness, ductility and durability are poor, making it difficult to serve for a long time [16]. High-performance concrete has high strength, but it also suffers from early cracking and poor fatigue life [17]. High-performance concrete containing fibers has the advantages of high strength and high mechanical properties [18]. However, the high cost and construction difficulty of high-performance concrete containing fibers limit its wide application [19]. Modified asphalt concrete improves the mechanical properties of asphalt to a certain extent, but the inherent rutting and crown appearance problems of asphalt are still serious and have not been solved yet [20] Epoxy resin concrete belongs to polymer concrete, which has good chemical resistance, low density and excellent mechanical properties. It is increasingly used in industrial and civil buildings [21]. It also has the advantages of rapid curing, good bonding performance and creep resistance [22], It can be used in the fields of bonding and repairing of concrete components, expansion joints, highway pavement, crack reinforcement of concrete structures, anti-seepage and plugging grouting [22,23].

This study proposes to design a steel slag self-compacting epoxy resin concrete (SERC) with steel slag as aggregate and epoxy resin as binder for road expansion joints, pavement repair and cement concrete crack repair. SERC is a special type of concrete that can be poured under its own weight and form strength without any vibration. By recycling steel slag, it reduces the use of natural aggregate, protects the natural environment, and can be used in practical projects. In this study, basalt epoxy resin concrete (BERC) with basalt as coarse aggregate and limestone as fine aggregate will be set as the control group to compare and verify the mechanical properties and road performance of SERC. SERC is mainly used for road expansion joints and pavement repair, so Marshall Design Method will be used to verify its mechanical properties and road performance. The formation mechanism of SERC and BERC strength will be revealed by elemental analysis and micro morphology. Mechanical test, road performance test and interlayer bonding test are used to study the differences in the mechanical properties and road performance between SERC and BERC. Furthermore, the physical engineering is carried out to verify the working performance and service performance of SERC.

2. Materials and experimental method

2.1. Materials

2.1.1. Epoxy resin binder

Epoxy resin binder included two components namely A and B. A component is epoxy resin, B component is curing agent. The technical properties are shown in Table 1.

2.1.2. Aggregates

The aggregates used were steel slag aggregate, basalt coarse aggregate (4.75 – 13.2 mm) and limestone fine aggregate (0 – 4.75 mm). The composition of oxides in steel slag aggregate, basalt coarse aggregate and limestone fine aggregate are shown in, Table 2, Table 3 and Table 4 and respectively.

The technical parameters of steel slag aggregate and basalt coarse aggregate are shown in Table 5 and Table 6 respectively, and the technical parameters of steel slag fine aggregate and limestone fine aggregate are shown in Table 7 and Table 8 respectively.

2.2. Design and preparation of epoxy concrete

2.2.1. Mixing ratio of epoxy resin

At room temperature, the components A and B were mixed uniformly in a mass ratio of 1:1. The technical properties of the binders obtained according to GB/T 2567–2008 are shown in Table 9.

2.2.2. Preparation of self-compacting concrete

The particle size range of basalt and steel slag is 4.75–9.5 mm, 9.5–13.2 mm. The size range of steel slag and limestone fine aggregate is 0–0.075 mm, 0.075–0.15 mm, 0.15–0.3 mm, 0.3–0.6 mm, 0.6–1.18 mm, 1.18–2.36 mm, 2.36–4.75 mm. The steel slag aggregate and basalt aggregate epoxy concrete have the same gradation curve, as shown in Fig. 1. When preparing self-compacting epoxy resin concrete, the components A and B were mixed evenly by mass ratio of 1:1 at room temperature, and then were poured into the mixing pot together with the aggregate in a mass ratio of 1:6 for stirring, and the stirring time was 50–70 s. The color of BERC was a faint grayish yellow, and the SERC was darker and brighter in appearance than the BERC.

2.2.3. Volume parameter

The volume parameters of the Marshall specimens of the formed SERC and BERC were tested, and the results are shown in Table 10.

2.3. Test method

2.3.1. X-ray fluorescence spectrometry (XRF)

Basalt, limestone and steel slag were ground into powder to make samples, which were tested by the basic parameter method. The X-ray tube emits primary X-rays to irradiate the samples to excite the fluorescent X-rays of the element to be measured. The fluorescent X-ray radiated from the sample passed through the spectroscopic crystal, and the X-ray fluorescence spectrum was dispersed into isolated monochromatic analysis lines. The intensity of each spectral line was measured by the detector, and converted into the element concentration according to the selected analysis method to obtain the element content of sample.

Table 2
The composition of oxides in steel slag.

Element composition	Fe_2O_3	CaO	SiO_2	MgO	MnO	Al_2O_3	P_2O_5	Others
Composition ratio	36.5 %	36.0 %	13.6 %	4.3 %	3.4 %	2.2 %	1.4 %	2.5 %

Table 3
The composition of oxides in basalt.

Element composition	SiO2	Fe2O3	CaO	AL2O3	MgO	TiO2	Na2O	Others
Composition ratio	39.9 %	19.2 %	15.9 %	10.6 %	10.0 %	2.0 %	1.9 %	0.4 %

Table 4
The composition of oxides in limestone.

Element composition	CaO	MgO	Fe_2O_3	SiO_2	MnO	P_2O_5	Al_2O_3	Others
Composition ratio	68.7 %	28.4 %	0.7 %	0.5 %	0.4 %	0.3 %	0.3 %	0.7 %

Table 5
Test results of steel slag technical parameters.

Test item	Test result	Technical index	Test method
Apparent relative density	3.60	≥2.5	JTG E42-2005T0605
Water absorption (%)	1.12	–	JTG E42-2005T0308
Crushing value (%)	13.6	≤28	JTG E42-2005T0316
Los Angeles wear value (%)	9.43	≤28	JTG E42-2005T0317

Table 6
Test results of basalt technical parameters.

Test item	Test result	Technical index	Test method
Apparent relative density	3.07	≥2.5	JTG E42-2005T0605
Water absorption (%)	1.08	≤2.0	JTG E42-2005T0308
Crushing value (%)	11.4	≤28	JTG E42-2005T0316
Los Angeles wear value (%)	8.1	≤28	JTG E42-2005T0317

Table 7
Test results of technical parameters of fine steel slag.

Test item	Test result	Technical index	Test method
Apparent relative density	3.60	≥2.5	JTG E42-2005T0605
Angularity (s)	52.86	≥30	JTG E42-2005T0308
Sand equivalent (%)	93.2	≥60	JTG E42-2005T0317

Table 8
Test results of limestone technical parameters.

Test item	Test result	Technical index	Test method
Apparent relative density	2.705	≥2.5	JTG E42-2005T0605
Angularity (s)	50.2	≥30	JTG E42-2005T0308
Sand equivalent (%)	83.78	≥60	JTG E42-2005T0317

Table 9
Technical properties of binders.

Initial cure time25°C/100 g (h)	Full cure time25°C/100 g (h)	Heat resistance (°C)	Tensile strength (MPa)	Bending strength (MPa)	Shear strength (MPa)
5	24	−60–120	16.08	30.47	12.14

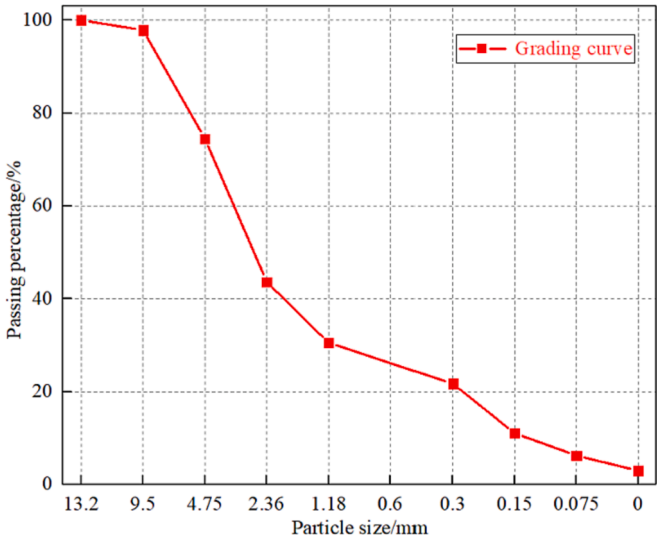

Fig. 1. Grading curve of aggregate.

Table 10
Volume parameters of SERC and BERC.

Material type	Maximum theoretical density	Gross volume relative density	Water absorption (%)	Porosity (%)	Marshall stability (kN)
SERC	2.516	2.454	0.21	2.5	21.5
BERC	2.185	2.136	0.19	2.2	42.3

2.3.2. *Scanning electron microscopy (SEM)*

The SERC and BERC samples were taken and tested by scanning electron microscope. Scanning electron microscope is an analytical instrument that uses secondary electrons and backscattered electron signals to obtain the morphology of the sample itself through vacuum system, electron beam system and imaging system, and its resolution can reach nanometer level.

2.3.3. *Cube compression test*

Four groups of cube samples were designed and prepared, and four parallel specimens were prepared for each group. and the sample size was 70.7 mm × 70.7 mm × 70.7 mm. The first group of SERC cubes were incubated at 15 °C, 25 °C, and 40 °C for 3 h, 6 h, 12 h, 24 h, 48 h, and 72 h respectively; The second group of BERC cubes were placed at 15 °C, 25 °C and 40 °C for 3 h, 6 h, 12 h, 24 h, 48 h and 72 h respectively; The third group of SERC cubes were left at −10 °C, 10 °C, 25 °C, 40 °C, 55 °C, and 60 °C for 6 h to form the final strength. The YES-2000 hydraulic pressure testing machine was used as the test instrument, and the samples were tested according to the test method of GB/T 50107–2000.

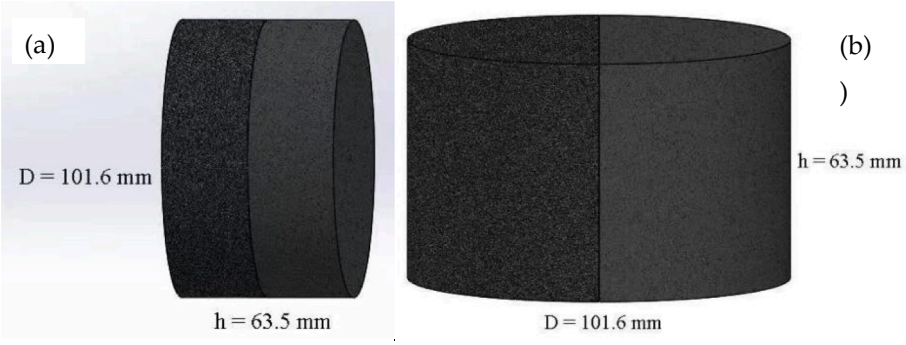

Fig. 2. Specimen combination forms. (a. interlayer bonding specimen, b. section bonding specimen).

2.3.4. Marshall stability test

Marshall specimens with a size of ϕ101.6 × h 63.5 mm were prepared with epoxy resin concrete, and four parallel test pieces were prepared for the experiment. then placed in a 25 °C incubator for incubate. The Marshall stability was tested after 3 h, 6 h, 12 h, 24 h, 48 h, and 72 h respectively.

2.3.5. Dynamic uniaxial compression test

Dynamic uniaxial compression tests were carried out to evaluate the high-temperature performance of epoxy resin concrete. Firstly, epoxy concrete samples of SERC and BERC with a size of ϕ 100 mm × h100 mm were prepared. The test was then carried out on a universal testing machine (UTM-100) at a temperature of 60 °C. The compressive stress was 0.7 MPa, using a half-sine waveform consisting of a loading time of 0.1 s and a rest time of 0.9 s. The test was automatically stopped when the vertical displacement reached 10 mm. The value of repeated loading times was used to evaluate the high temperature stability of epoxy resin concrete.

2.3.6. Rutting test

Prepare three rut specimens with a size of 300 mm × 300 mm × 50 mm and incubated at 25° C for 3 days. Before the test, the specimens were conditioned at a constant temperature for more than 5 h, and the test temperature, wheel load, and speed were 60 °C, 0.7 MPa, and 42 times/min, respectively.

2.3.7. Semi-circular bending test (SCB)

The SCB test was used to test the low temperature performance. The specimens used were Marshall specimens with a size of ϕ 101.6 mm × h 63.5 mm. The semi-circular was cut evenly with a seam depth of 10 mm and a seam width of 4 mm. The specimens were next placed in a −10 °C incubator for 4–6 h. The specimen was placed on the support of the UTM testing machine, loaded at a rate of 1.27 mm/min until the specimen failed, and the test was stopped when the load stress fell below 0.1 kN. In this experiment, four parallel specimens are designed for testing.

2.3.8. Low temperature trabecular test

Trabecular specimens with a size of 250 mm × 25 mm × 30 mm were used for the low-temperature trabecular test, and the trabecular specimens were placed at −10 °C, 5 °C, and 20 °C for 5 h to ensure that the internal temperature of the specimens reached the ambient temperature. The specimens were tested by UTM-100 after the holding time. In this experiment, four parallel specimens are designed for testing.

2.3.9. Freeze-thaw split test

Referring to the T 0729–2000 freeze–thaw splitting test in JTG E20-2011, two groups of epoxy resin concrete Marshall specimens were prepared. Taking one group as the test condition group, the specimens were subjected to vacuum pumping, atmospheric pressure static, −16 °C low-temperature freezing and other operation steps, while the other group was taken as the non-condition group. In this experiment, four parallel specimens are designed for testing.

2.3.10. Water immersion Marshall test

Referring to the T 0709–2011 immersion Marshall test in JTG E20-2011, two groups of epoxy resin concrete Marshall test pieces were prepared. One group was subjected to the standard Marshall test, and the other group as the test condition group was kept in a constant temperature water bath at 60 °C for 48 h, the rest of the operation steps were the same as the standard Marshall test method. In this experiment, four parallel specimens are designed for testing.

2.3.11. Repeated-loading semicircular bending test (R-SCB)

The Marshall specimens to be subjected to fatigue test shall be cut in the middle of the bottom to form a semicircle and ensure that the position and depth of the slits in the same batch were the same. The fatigue tests shall be carried out with different stress levels respectively, and the number of actions when the specimens reach the failure state shall be recorded. The stress level ratios used in the test were 0.4, 0.5, 0.6, 0.7 and 0.8.

2.3.12. Interlayer bonding performance test

Marshall specimens of half AC–13 asphalt mixture and half AC-16, SERC or BERC (i.e. AC-13–AC-16, SERC–AC-13, BERC–AC-13) were made according to the combination form as shown in Fig. 2(a), and tested with a UTM for testing the interlayer properties of epoxy resin concrete. Marshall specimens of half AC-13 asphalt mixture and half SERC or BERC (AC-13, SERC–AC-13, BERC–AC-13) were made according to the combination form as shown in Fig. 2(b), and the splitting strength of SERC and BERC was tested with a Marshall Stability Tester. In this experiment, four parallel specimens are designed for testing.

3. Test results and discussion

3.1. Strength formation mechanism of self-compacting epoxy resin concrete

3.1.1. Elemental analysis

In addition to the mechanical bite force formed on the aggregate surface after the epoxy resin was cured, there was a second force in epoxy resin concrete. According to coordination bond theory [24], existence of strong polarity of binder molecules will form shared electron pairs with the bonded material, resulting in coordination bonds. Epoxy resin curing compound has 3 groups, the hydroxyl group, the ether bond and the epoxy group [25]. The C element in the epoxy benzene ring could be chemically shifted to form ligands with Ca and Si elements [26]. Based on the above-mentioned research, this study carried out XRF tests to test the major elemental compositions in the three aggregates to explain the differences in the strength formation rates between SERC and BERC in terms of coordination bonds.

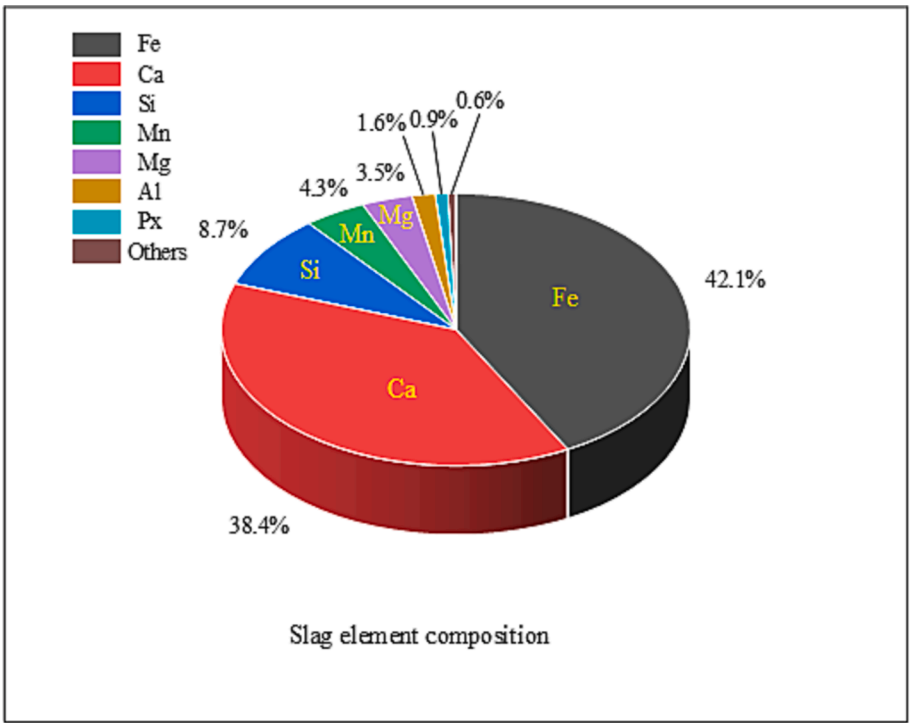

Fig. 3. Elemental composition of steel slag.

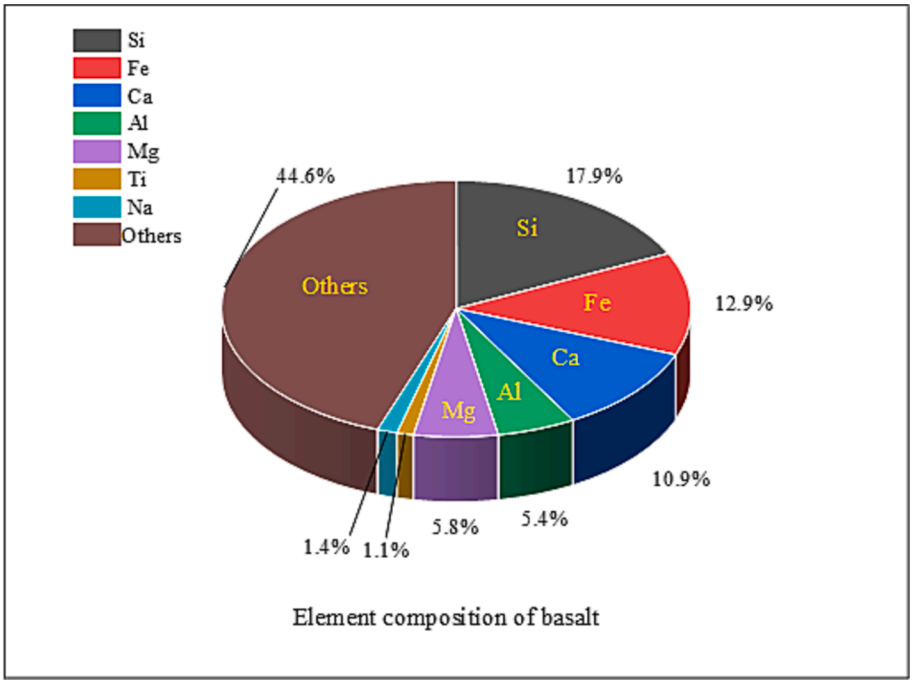

Fig. 4. Element composition of basalt.

The elemental compositions of steel slag, basalt and limestone are shown in Figs. 3–5 respectively. As can be seen from the figures, the steel slag is mainly composed of Fe, Ca, Si, Mn and Mg, the basalt is mainly composed of Si, Fe, Ca, Al and Mg, and the limestone is mainly composed of Ca, Mg, Fe, Si and Mn. Ca plus Si in steel slag is 47.1 % of the sum of all elements, while Ca plus Si in basalt and limestone are 28.8 % and 20.1 % of the sum of all elements respectively. The proportion of impurity elements in steel slag is very small at 0.6 %, while the proportion of impurity elements in basalt and limestone at 44.6 % and 37.8 % respectively. Steel slag is an industrial by-product of high-temperature steelmaking at temperatures as high as 1500–1700 °C [27]. Many impurity elements were deliberately removed during the steelmaking process due to the steelmaking process requirements, and some elements were removed after forming oxides at high temperature. Limestone and basalt are quarried from mountains and have not been subjected to high temperatures [28] and industrial deliberate removal of impurity elements. Therefore, basalt and limestone contain more impurity elements than in steel slag, with Si and Ca accounting for a lower

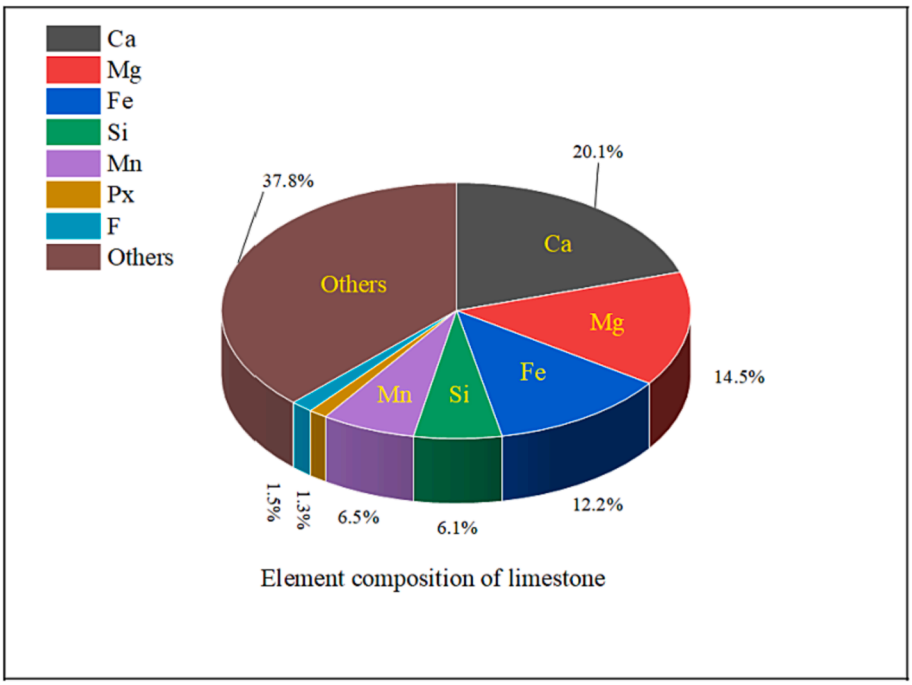

Fig. 5. Elemental composition of limestone.

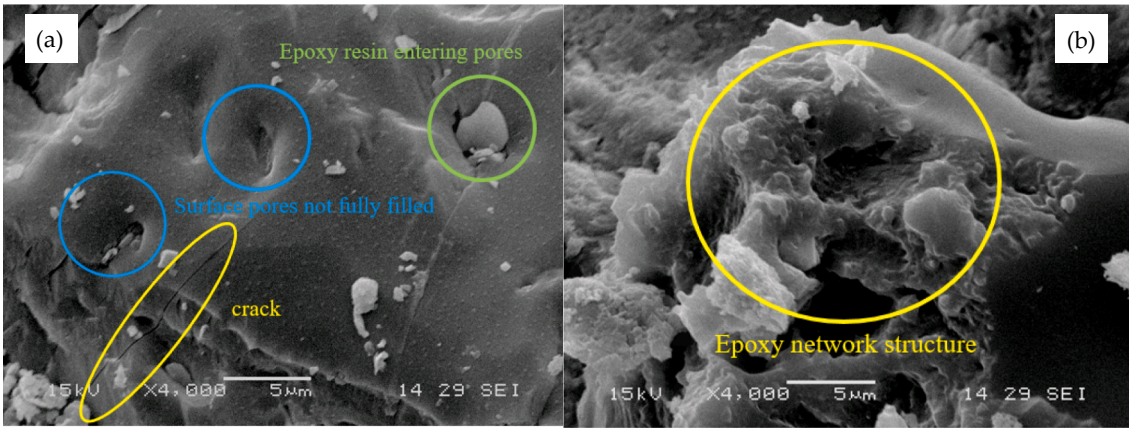

Fig. 6. (a. SEM image of SERC; b. SEM image of BERC).

percentage.

The aggregates of SERC consist of steel slag coarse aggregates and steel slag fine aggregates, and the aggregates of BERC consist of basalt coarse aggregates and limestone fine aggregates. The sum of Si and Ca element in steel slag accounts for 47.1 % of the total elements and only accounts for 20.1 % in limestone. C in the epoxy resin benzene ring mainly formed coordination bonds with Si and Ca elements, and Si and Ca in coarse and fine steel slag were in more contact with the epoxy resin benzene ring, so its coordination bond formation rate was faster, and its bond strength formation rate was faster, making the early strength formation rate of SERC greater than that of BERC.

3.1.2. Surface micromorphology

The SEM scans of SERC are shown in Fig. 6(a), and the SEM scans of BERC are shown in Fig. 6(b). From Fig. 6(a), it can be seen that the SERC epoxy resin film uniformly wrapped the steel slag aggregate, forming a three-dimensional cross-linked network structure [29]. There were pores on the concrete surface and the epoxy resin did not completely fill the open pores on the steel slag surface, and micro-cracks were generated on the surface. As shown in Fig. 6(b), the BERC surface was completely encapsulated by the epoxy resin and formed a three-dimensional cross-linked network structure.

Epoxy resin is a typical thermosetting material, and after curing it presents a highly cross-linked structure with little plastic deformation. The reduction of volume shrinkage will generate certain internal stress, which will tear the epoxy resin film and form certain micro cracks [30]. The steel slag used in this study was an industrial by-product with a rough and porous surface. The mix ratio showed that SERC contained 3 % of steel slag micronized powder in the range of 0–0.075 mm and the sum of Si and Ca elements was as high as 47.1 %, while the sum of Si and Ca elements in limestone micro powder was only 20.1 %. Thus, the slag micronized powder exhibited certain activity and formed coordination bonds with the C element in the benzene ring of the epoxy resin group. Research shows that the active micro powder can interact with the epoxy resin and form a good interface between the aggregate and the epoxy resin [31]. The internal stress pushes the steel slag micronized powder around and creates micro cracks in the epoxy matrix, thus absorbing energy to increase the toughness of the epoxy matrix [32].

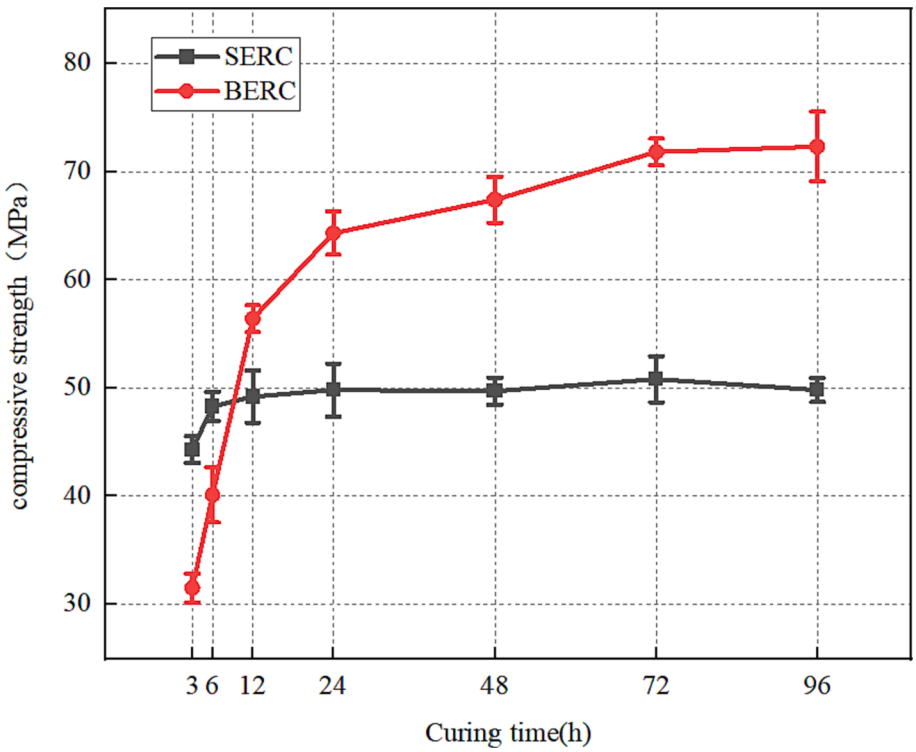

Fig. 7. Compressive strength and curing time of SERC and BERC cubes.

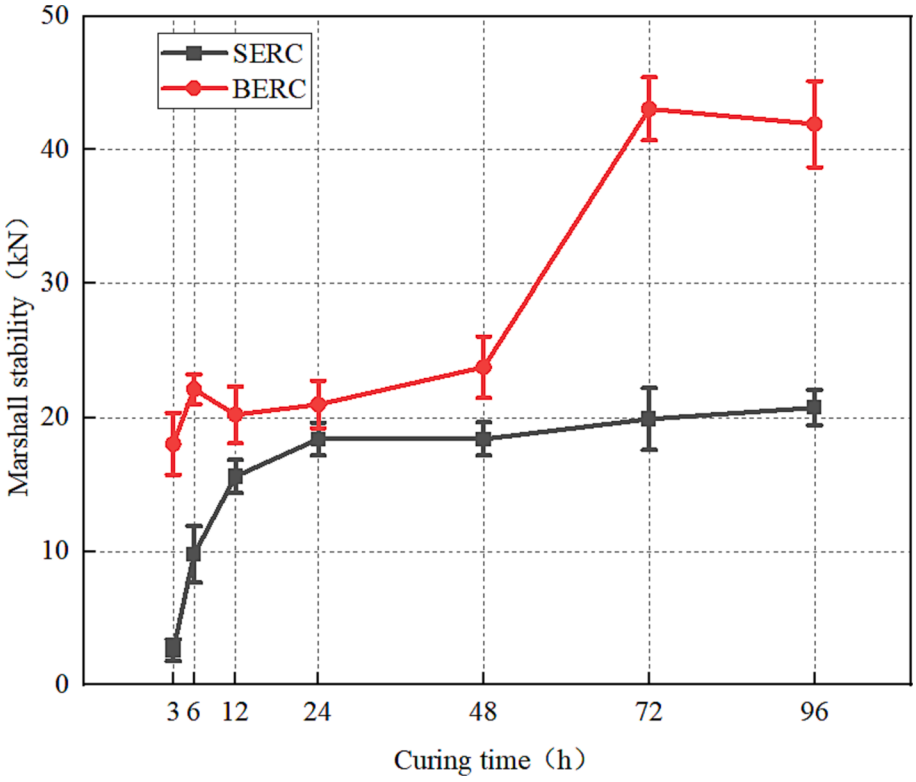

Fig. 8. Marshall Stability and curing time of SERC and BERC.

The epoxy film thickness is an important factor affecting its strength and other properties, when the film thickness is thicker, the bonding force between the aggregates is greater and its strength is greater [33]. The surface openings of limestone and basalt are relatively smooth and the open pores are less than those of steel slag with the same particle size, meaning that more aggregate pores in SERC at the same ratio absorb more epoxy resin, so the thickness of the epoxy film of SERC was lower than that of BERC [34]. BERC had a thicker epoxy resin film thickness and therefore more resistant to internal stresses caused by resin shrinkage, with fewer or no micro-cracks caused by stress shrinkage.

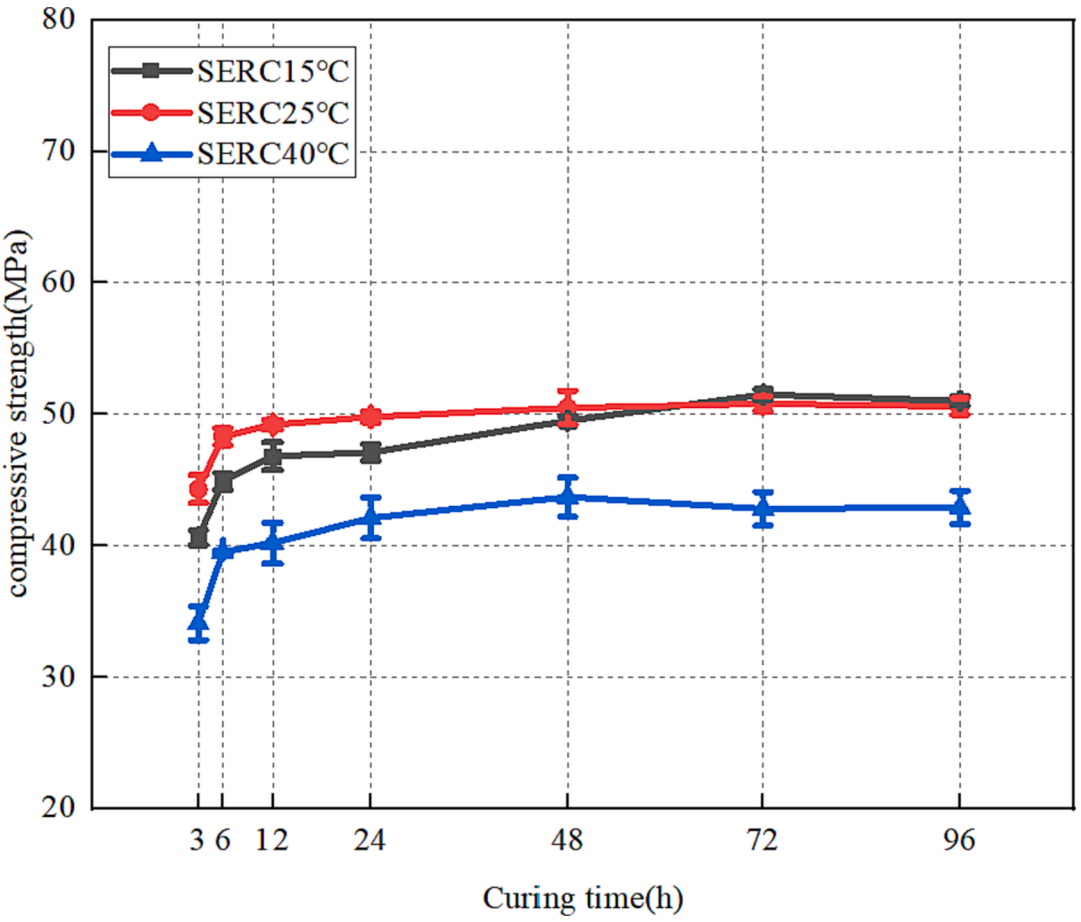

Fig. 9. SERC strength at different curing temperatures.

SERC had a thin epoxy resin film, which was less resistant to internal stress and has more cracks due to stress contraction, and the activity of steel slag micronized powder was higher than that of limestone micronized powder. As a result, there are more micro cracks on the surface of SERC than BERC, resulting in a better toughness of SERC than BERC.

3.2. Factors affecting the mechanical properties of self-compacting concrete

3.2.1. The effect of curing time on strength formation

Cube compressive strength and Marshall Stability tests were carried out to investigate the effect of curing time on the compressive strength of SERC and BERC. The cubic compressive strength and Marshall stability of SERC and BERC were tested at 3 h, 6 h, 12 h, 24 h, 48 h, 72 h and 96 h under curing conditions at 25 °C. The test results are shown in Fig. 7 and Fig. 8. The cubic compressive strength and Marshall Stability of both epoxy concretes became greater with increasing curing time until final strength was developed. The SERC basically formed the final strength at 12 h, and still had a small increase after 12 h, while the BERC developed its final strength at 72 h. The compressive strength of SERC cubes was 37.2 % and 20.3 % higher than that of BERC cubes at 3 h and 6 h respectively. The final cubic compressive strength of SERC was 51.2 MPa, which was 29.2 % lower than that of BERC. The Marshall Stability and cube compressive strength of the two epoxy concretes showed a similar pattern. The Marshall stability values of SERC remained essentially stable at 12 h, and increased slightly after 12 h. The Marshall stability of SERC was 19.8 MPa, which was 41.9 % lower than that of BERC.

From the above analysis, it can be concluded that both epoxy resin concretes had good mechanical properties. The thickness of the epoxy resin film in BERC was greater than that of SERC, and there were differences in the aggregate elements of SERC and BERC, resulting in a lower early strength of BERC than SERC. Although the cubic compressive strength and the final strength of Marshall Stability of SERC were only 68.1 % and 49.2 % of BERC respectively, its cubic compressive strength reached 50.0 MPa, which was equivalent to the strength of C50 cement. The early strength of SERC was higher than that of BERC, and the final strength formation time was 83.3 % less than that of BERC. Therefore, SERC is more suitable than BERC for road sections that require rapid traffic development. The epoxy film of BERC was thicker and the crushing and abrasion values of basalt were smaller than those of steel slag, which made the final strength of BERC greater than that of SERC.

3.2.2. The effect of curing temperature on strength formation

The cube specimens of two kinds of epoxy resin concrete were cured at 15 °C, 25 °C and 40 °C respectively, and the curing time was 3 h, 6 h, 12 h, 24 h, 48 h, 72 h and 96 h respectively. The influence of curing temperature on strength formation was explored by testing the cube compressive strength under different curing temperatures. The SERC test results are shown in Fig. 9 and the BERC test results are shown in Fig. 10. Under the curing conditions of 15 °C, 25 °C and 40 °C, the final strength of SERC was formed at about 12 h. The final strength under 15 °C and 25 °C curing was almost the same. The final strength of curing at 40 °C was 13.4 % less than that at 15 °C. The final strength formation of BERC under three curing temperatures was formed at about 72 h. Under the same curing temperature, the final strength of SERC was 28.6 % lower than that of BERC.

According to the above analysis, the compressive strength of the two

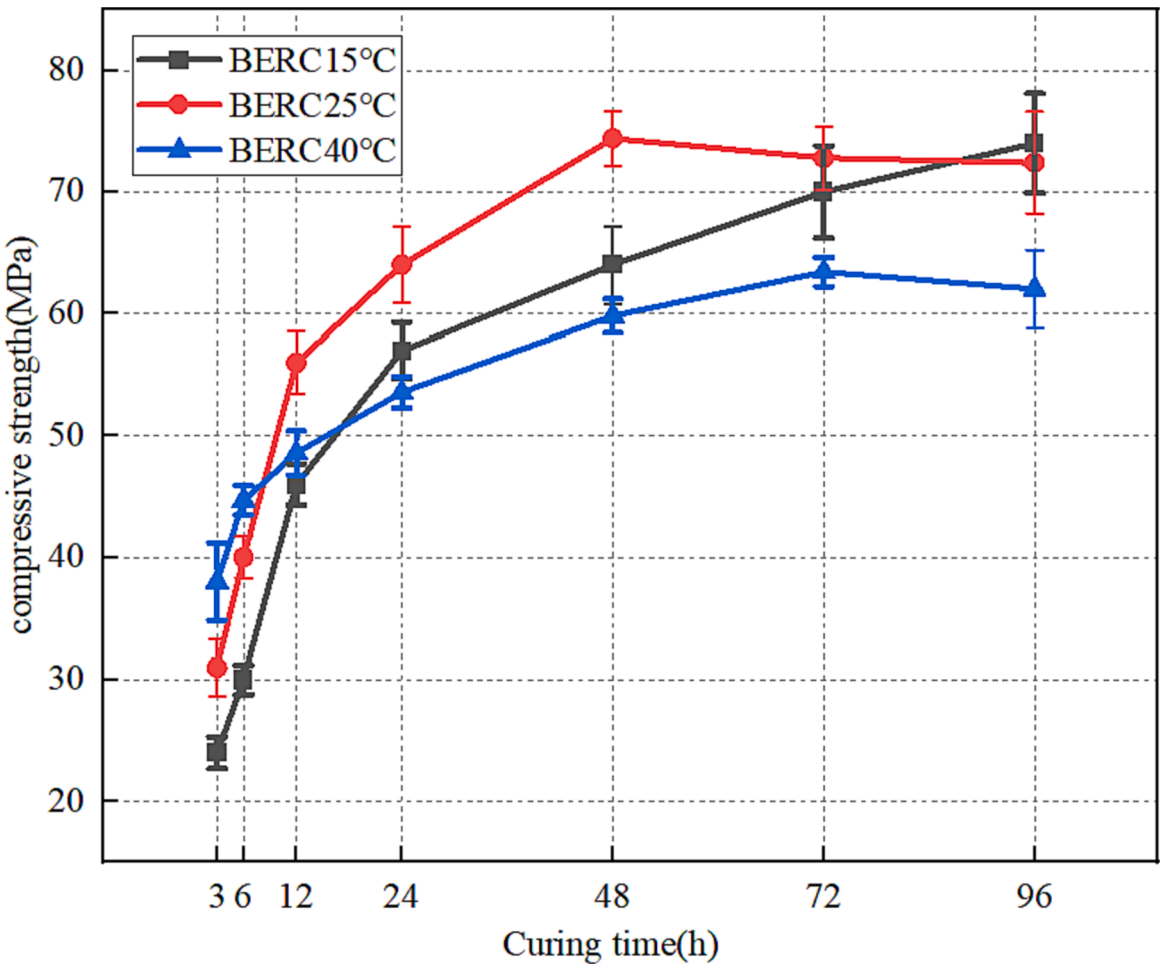

Fig. 10. BERC strength at different curing temperatures.

kinds of epoxy resin concrete under different curing temperatures showed a similar law. The strength of the two kinds of epoxy resin concrete under different curing temperatures increased with the growth of curing time until the final strength was formed. The formation time of the final strength of epoxy resin concrete was related to the type of concrete and curing time, but had nothing to do with the curing temperature. Different curing temperatures leaded to the different final strength, and the difference in final strength formed at 15 °C and 25 °C was very small. The final strength formed at 40 °C curing temperature was 13.4 % smaller than that at 15 °C and 25 °C curing temperatures. To sum up, the optimal curing temperature for SERC and BERC was 25 °C.

3.2.3. Effect of temperature on strength

It can be seen from section 3.2.2 that the final compressive strength formed at 40 °C curing temperature had a large difference with the cubic compressive strength formed at 25 °C and 15 °C curing temperatures. When performing strength tests at different curing temperatures, in order to control the curing duration, the cubic specimens taken out from the thermostat were directly tested, and the temperatures of the specimens during the test were different. In order to find out whether the reason for the difference of final strength under 40 °C, 25 °C and 15 °C curing conditions was the difference of curing temperatures or the internal temperatures of the specimens during testing, and to explore the influence of service temperature on the strength of epoxy resin concrete, the experimental study of the influence of temperature on the strength was supplemented.

After the strength has been fully formed, the two kinds of epoxy resin concrete cube specimens were placed in the incubator at −10 °C, 10 °C, 25 °C, 40 °C, 55 °C and 70 °C for curing for more than 4 h. When the internal temperature of the specimens reached the temperature of the curing environment, the compressive strength test was carried out immediately, and the test data is shown in Fig. 11. It can be seen that the overall trend of compressive strength of both epoxy concrete decreased with increasing temperature. The compressive strengths of the two epoxy concretes changed little from −10 °C to 25 °C, and began to decrease significantly when the temperature reached 40 °C, indicating

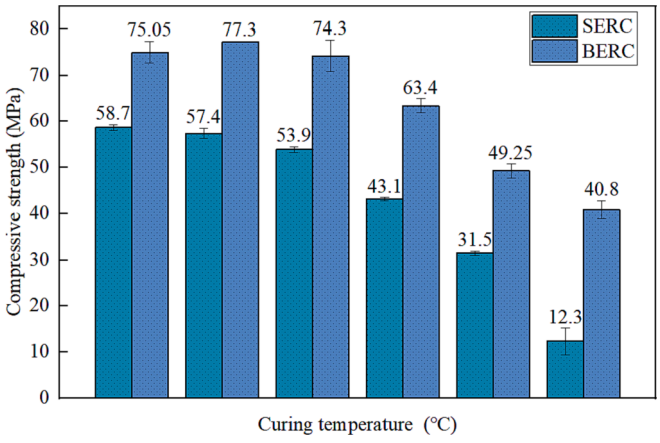

Fig. 11. Relationship between compressive strength and temperature of SERC and BERC.

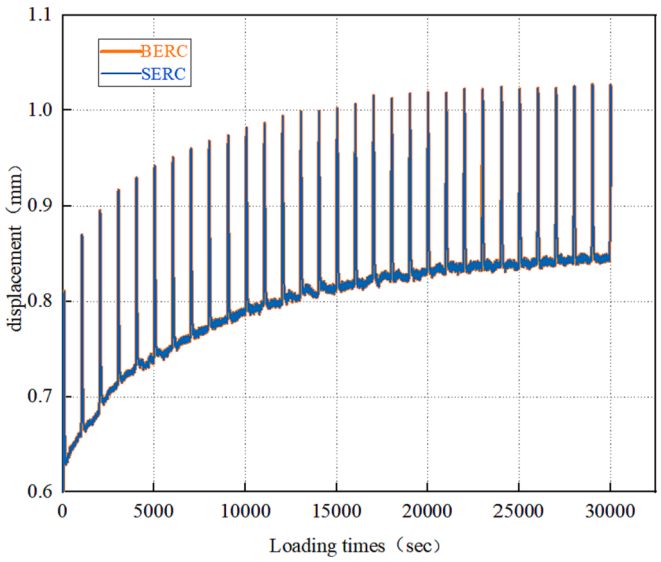

Fig. 12. Variation curve of SERC and BERC displacement with loading times.

that the service temperature had a greater effect on the compressive strength of epoxy concrete, and the regeneration temperature had less effect on the final strength formation of SERC and BERC. At the same time, the decrease of SERC was greater than that of BERC, and the cubic compressive strength of SERC was lower than that of BERC at the same temperature. The compressive strength of BERC was better than that of SERC in general, and the strength advantage of BERC was more obvious at high temperatures, but SERC also had relatively high strength.

3.3. Road performance of self-compacting epoxy resin concrete

3.3.1. Research on the high temperature stability

Dynamic uniaxial compression test and rutting test were used to evaluate the high temperature stability of the specimens. The dynamic uniaxial compression test simulated the load of 0.7 MPa and repeatedly loaded the specimen more than 30,000 times. As shown in Fig. 12, the deformation amplitude of the SERC and BERC specimens loaded for 30,000 times was only 0.21 mm, and there was no obvious deformation or crack on the surface of the SERC and BERC specimens. It indicated that the specimens were not structurally damaged. Moreover, the loading times and deformation curves of BERC almost coincided with that of SERC, so it was impossible to judge the difference in the high temperature performance between the two epoxy resin concretes. It showed that loading 30,000 times was far from the loading times required for the failure of the specimen. It can be seen from the literature that the asphalt concrete specimens will be structurally damaged when the loading times reaches 5000 in the dynamic uniaxial compression test [35,36], which is far less than the loading times of SERC and BERC. In conclusion, SERC and BERC have excellent high temperature stability.

As shown in Fig. 13, the dynamic stability of BERC was 47.61 % higher and the rut depth was 40 % lower than that of SERC. The high temperature stability of epoxy resin concrete is actually the ability to resist deformation at high temperature. The deformation of epoxy resin concrete is mainly the deformation of cementitious material, which changes the internal structure of concrete. Its high temperature stability was mainly related to the physical properties of the binder and aggregate itself. It can be seen from Fig. 11 that the compressive strength of BERC at 55 °C and 75 °C was greater than that of SERC, indicating that its ability to resist deformation at high temperature was better than that of SERC. The epoxy resin binder in SERC had better high temperature stability than SEEC because the steel slag micro powder increased its toughness, while its strength decreased. The dynamic stability of SERC was more than 25,000 times/mm, the rut depth was only 0.025 mm, and the high-temperature performance was far better than that of asphalt concrete [37], which was sufficient for expansion joints and other purposes.

3.3.2. Research on the low temperature cracking resistance

The low temperature performance of two groups of epoxy concretes were characterized by semi-circular bending test and low temperature trabecular test. Fig. 14 and Fig. 15 show the displacement versus load curves and fracture energy of the SCB test respectively. It can be seen from Fig. 14 that the load of the SERC specimens at fracture was 33.3 % higher than that of the BERC, and the deformation of the SERC was 9.8 % lower than that of the BERC, while it can be seen from Fig. 15 that the fracture energy of SERC was 37.1 % higher than that of BERC, which showed that SERC had better low temperature cracking resistance than BERC.

Fig. 16 shows the flexural tensile strain data of SERC and BERC. It can be seen that the flexural tensile strain of SERC was 2794.6 με at −10 °C, 9.2 % lower than that of BERC at 5 °C and 22.7 % higher than that of BERC at 20 °C. Fig. 17 shows the bending stiffness modulus data of SERC and BERC. It can be seen that the bending stiffness modulus of SERC was 8651.2 MPa at −10 °C, which was 43.3 % and 55.0 % lower than that of BERC at 5 °C and 10 °C respectively. And the data of BERC

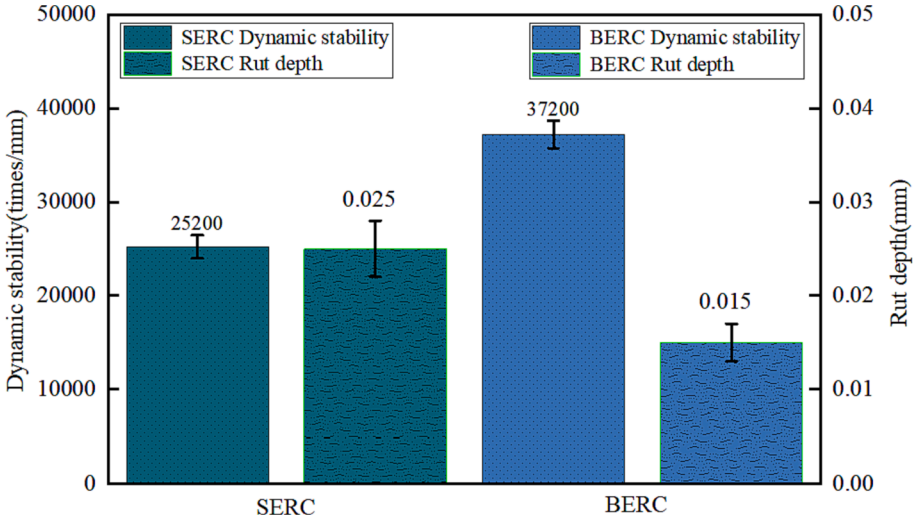

Fig. 13. The rutting test results of SERC and BERC.

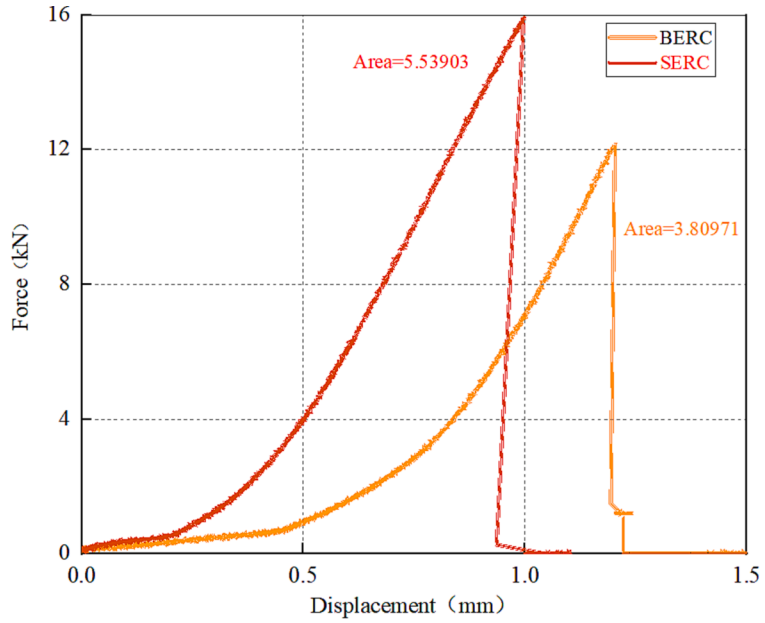

Fig. 14. Relation curve between displacement and load of SERC and BERC.

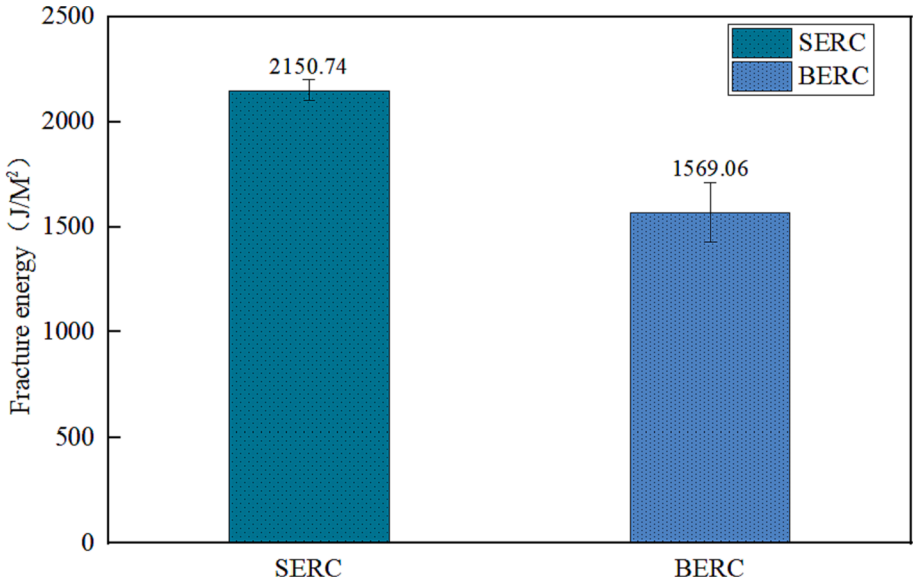

Fig. 15. Fracture energy of SERC and BERC.

could not be measured at −10 °C, indicating that BERC has poor low temperature crack resistance. The crack resistance of BERC at 5 °C and 20 °C was also not as good as SERC. Combined with SCB test and low temperature trabecular test, it was found that steel slag micro powder enhanced the toughness of epoxy resin in SERC, so its crack resistance at low temperature was better than that of BERC.

The low temperature trabecular experiment generally tests the flexural tensile strain and flexural stiffness modulus of trabecular specimens at −10 °C to characterize the low temperature performance of the specimens. Because the BERC low-temperature trabecular specimens after being kept at −10 °C for 5 h will be brittle and fractured in the preloading stage of UTM-100, and the corresponding data cannot be obtained, trabecular tests at 5 °C and 20 °C were set up in this study. While the desired data of SERC can be measured by UTM-100 at −10 °C, so the trabecular tests at-10 °C, 5 °C and 20 °C were set up in this study.

3.3.3. Research on the water damage resistance

The test results of freeze–thaw split test and immersion Marshall Test are shown in Fig. 18 and Fig. 19 respectively. It can be seen from Fig. 18 that the TSRs of SERC and BERC were both greater than 100 %, indicating that both epoxy resin concretes have good water damage resistance. As higher temperature will accelerate the curing of epoxy resin, Marshall specimens in the test condition group were placed in a constant temperature water bath at 60 °C for 24 h, and it was found that the strength formation rate inside the specimen was higher than that of the Marshall specimens placed at room temperature. However, the final test temperature of the freeze–thaw split test was 25 °C, resulting in a slightly higher fatigue strength of the freeze–thaw specimens than that of the unfrozen specimens (see Fig. 20).

It can be seen from Fig. 19 that the residual stability of SERC in water was 6.1 % lower than that of BERC. It can be seen from section 3.1.2 that there were many micro-cracks on the surface of the SERC, and the

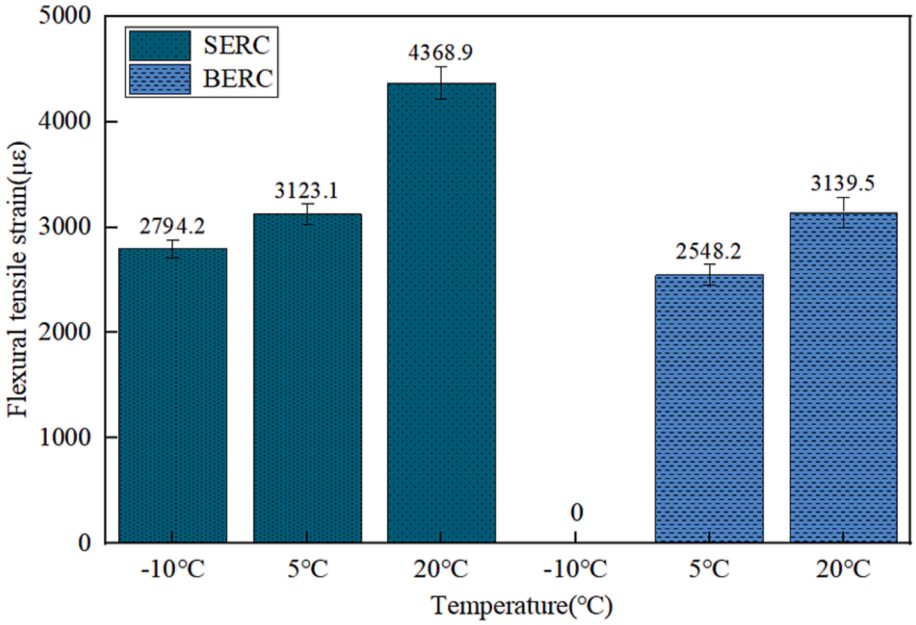

Fig. 16. Bending tensile strain of SERC and BERC.

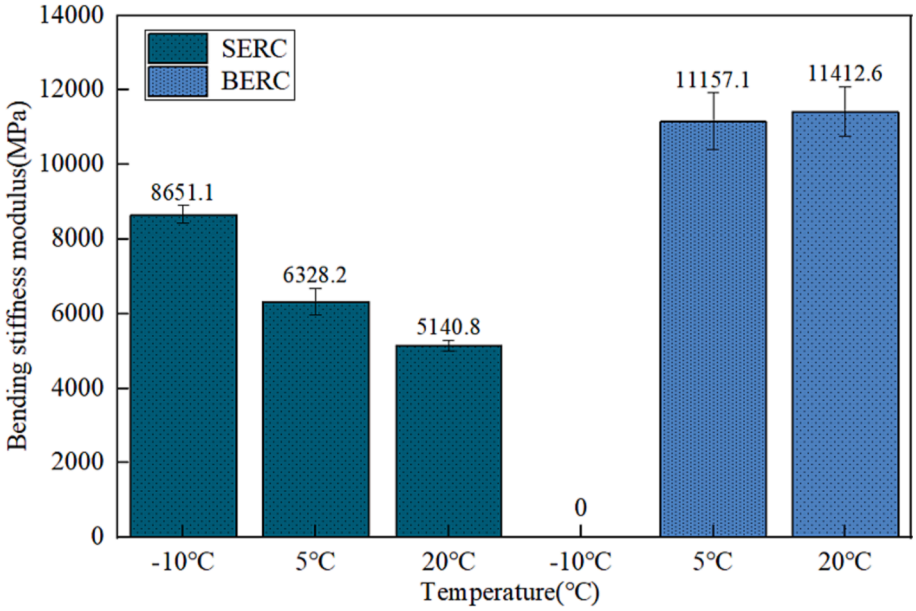

Fig. 17. Bending stiffness modulus of SERC and BERC.

activity of water molecules at 60 °C was more intense than that at room temperature [38], so in this case, water molecules would enter the interior of the SERC from the micro-cracks, causing certain damage to the interior. While epoxy resins are highly tough materials, so water molecules can not cause severe structural damage to the SERC. There were few micro-cracks on the surface of the BERC and the epoxy resin has formed a three-dimensional network structure, so it was difficult for water molecules to enter the interior of the BERC, and it was difficult to cause actual damage to BERC with a small molecular weight of water. From the comprehensive freeze–thaw splitting test and immersion Marshall Test, it can be concluded that both SERC and BERC have relatively good water damage resistance, and the water damage resistance of BERC was better than that of SERC.

3.3.4. Research on the fatigue resistance

Fig. 23 shows the relationship between fatigue life and stress level of SERC and BERC, which was fitted by the relationship between fatigue failure times and stress ratio obtained from the R-SCB test. It can be seen from the figure that the fatigue life curves of the two epoxy resin concretes were relatively close, and the regression coefficient between the logarithmic fatigue life and the stress level reached more than 0.98, so the fatigue life equation can well predict the fatigue life of the two. In contrast, the loading times of SERC in each stress ratio were greater than that of BERC, and the slope of BERC was slightly larger than that of SERC, indicating that the fatigue resistance of SERC was better than that of BERC. It can be concluded that SERC has higher toughness than BERC, that is, SERC has better fatigue resistance.

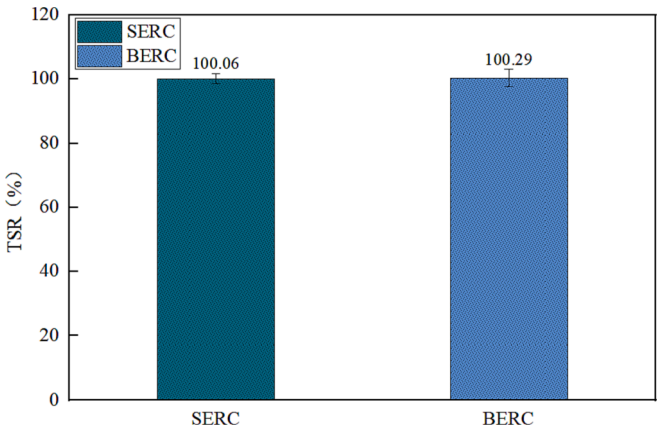

Fig. 18. Freeze-thaw splitting ratio of SERC and BERC.

3.4. Interlayer bonding properties of self-compacting epoxy resin concrete

3.4.1. Research on the interlayer bond strength

The interlayer test specimens were standard Marshall test specimens made by directly superimposing epoxy resin on the 30 mm high asphalt mixture Marshall test specimens. The specimens in this test were SERC–AC-13, BERC–AC-13 and AC-20–AC-13, and the fabricated interlayer specimens were loaded along $\theta = 90°$. As shown in Fig. 21, the inter-laminar shear strength of SERC–AC-13 was 12.8 % lower than that of BERC–AC-13 and 78.3 % higher than that of AC-13–AC-16. It can be concluded that the bond strength between both epoxy resin concretes and the original asphalt pavement was relatively good, and the interlayer bond performance of BERC was better than that of SERC.

3.4.2. Research on the cross-section bond strength

The cross-section bond strength was evaluated by the cross-section bond test. The AC-13 asphalt mixture Marshall Specimen was cut into a semi-circular to expose the cross-section, and then used a mold to bond the epoxy resin concrete to the semi-circular to form a complete Marshall Test specimen. In this experiment, SERC–AC-13, BERC–AC-13 and AC-13 specimens were made, and their splitting strength was measured by the splitting fixture of the Marshall Stability tester.

As shown in Fig. 22, the splitting strength of SERC + AC-13 is not much different from that of BERC + AC-13. The splitting strength of SERC + AC-13 is 2.5 % higher than that of BERC-AC-13 and 69.8 % higher than that of AC-13. Both SERC–AC-13 and BERC–AC-13 were specimens rebonded after damage, and their splitting strength was higher than that of the Marshall specimens of undestroyed AC-13, indicating that both epoxy resin concretes have good adhesion to asphalt mixture cross-section. When SERC and BERC are used as concrete fillers for expansion joints, they have good adhesion to the bridge boundary, which can effectively prevent water damage caused by the separation of expansion joint fillers from the original interface, thereby improving the physical properties and durability of expansion joints.

3.5. Practical engineering verification of SERC

In order to verify the feasibility and practical performance of SERC as an expansion joint, a certain part of a highway under construction in Hubei Province of China was selected as the test section of the expansion joint on the basis of the indoor test. SERC has the characteristics of easy mixing, good construction and workability. After the surface is smoothed, the SERC has good flatness, and there is no obvious gap between the expansion joint and the original road surface after filling. Fig. 23 shows the SERC expansion joint one year after of the opening to traffic. It can be seen from Fig. 23(a) that the SERC expansion joint after one year of operation was smooth and had no obvious disease. Fig. 23(b) shows that the silicone in the SERC expansion joint was seriously deformed and has poor contact with the SERC, which was mainly due to the performance of the silicone itself and had nothing to do with the performance of the SERC. As shown in Fig. 23(c), the surface of the SERC expansion joint was smooth without pits and obvious cracks, and had good contact with the original asphalt pavement. Due to practical engineering limitations, the BERC expansion joint test section was not set up. The actual road performance of the SERC expansion joint was considered with reference to the ultra-high performance cement concrete (UHPC) expansion joint that has been open to traffic for one year on a highway in Hubei. As shown in Fig. 24(a), the surface of the UHPC expansion joint had a flat appearance, and the overall structure was intact and undamaged. As shown in Fig. 24(b), the surface of UHPC had small potholes and poor contact with the original pavement. As shown in Fig. 24(c), the surface of the UHPC expansion joint had small-scale concrete breakage and many micro-cracks distributed.

Both SERC and UHPC can be used as expansion joints. Although the UHPC expansion joint has problems such as micro-cracks on the surface, poor adhesion with the road surface, and small-scale concrete breakage,

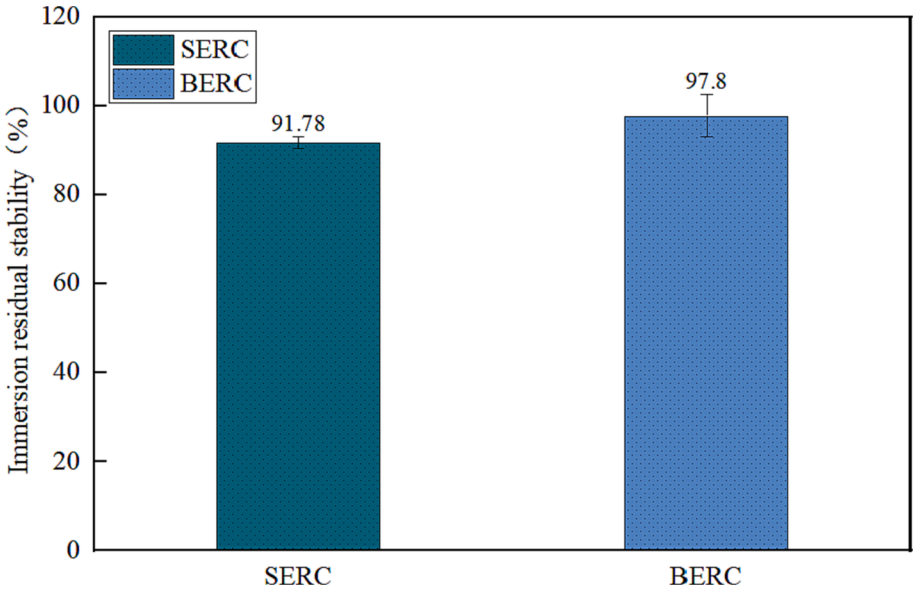

Fig. 19. Immersion residual stability of SERC and BERC.

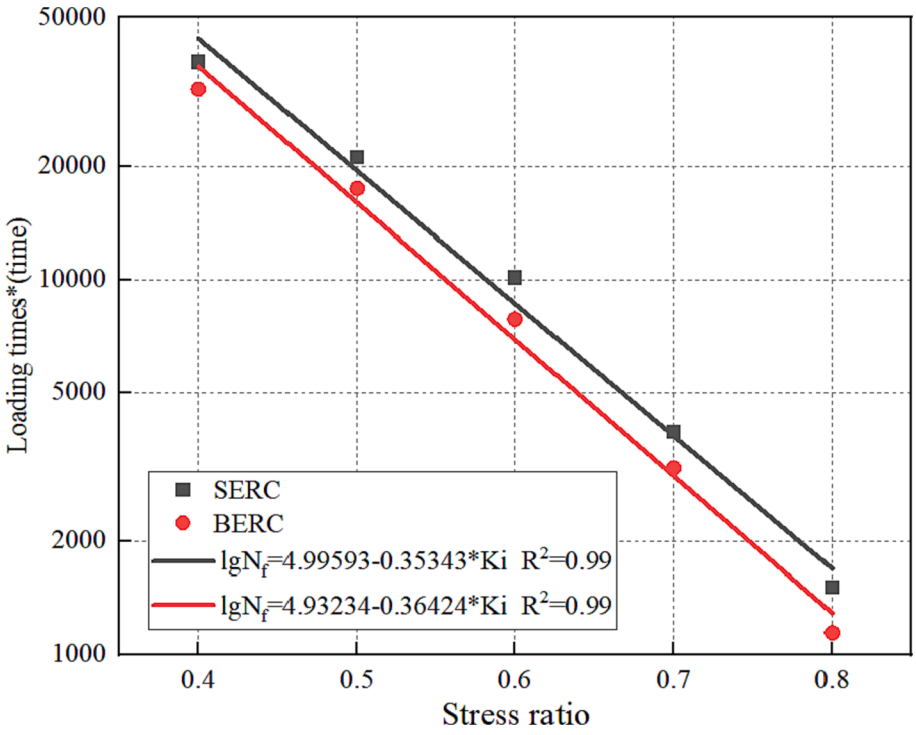

Fig. 20. Relationship between fatigue life and stress level of SERC and BERC.

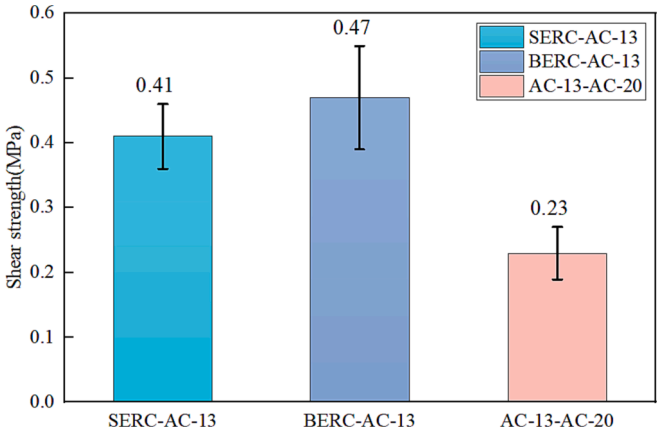

Fig. 21. Bond strength between layers of SERC and BERC.

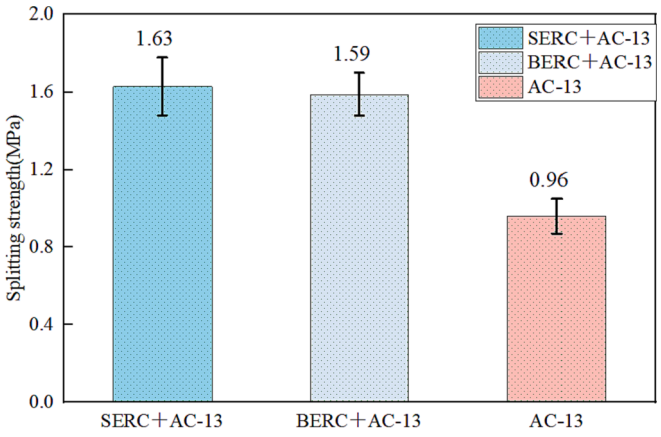

Fig. 22. The splitting strength of SERC and BERC.

the structure was complete as a whole, and the road performance was not actually affected. After one year of service, the SERC expansion joint had a complete structure and no obvious disease, so it can absolutely be used as an expansion joint.

4. Conclusion

Based on the study of mechanical properties and micro mechanism, the reasons for the difference in formation rate and final strength between SERC and BERC were analyzed, and then the mechanical properties of SERC and BERC were verified by a series of tests. Finally, it was verified by the actual test road section. The following conclusions can be drawn:

(1) The high content of Si and Ca in SERC and BERC aggregates leaded to fast strength formation rate. The micro cracks in the epoxy matrix in SERC toughen SERC, which made the low-temperature performance and fatigue of SERC better than that of BERC. The thicker epoxy film thickness of BERC and the greater hardness of aggregate made the strength of BERC better than that of SERC.

(2) Both SERC and BERC had excellent mechanical properties. The formation time of final strength was related to the curing time, but has nothing to do with the curing temperature. The strength of SERC and BERC was different at different temperatures, and decreased with the increase of temperature. The early strength of SERC was higher than that of BERC, and the strength formation speed was faster than that of BERC, but the final strength of BERC was higher than that of SERC. SERC had high strength and fast forming speed. SERC formed the final strength at 24 h and BERC formed the final strength at 72 h.

(3) SERC and BERC have excellent high temperature stability, water damage resistance and fatigue resistance. SERC has good low temperature cracking resistance, while BERC has poor low temperature cracking resistance.

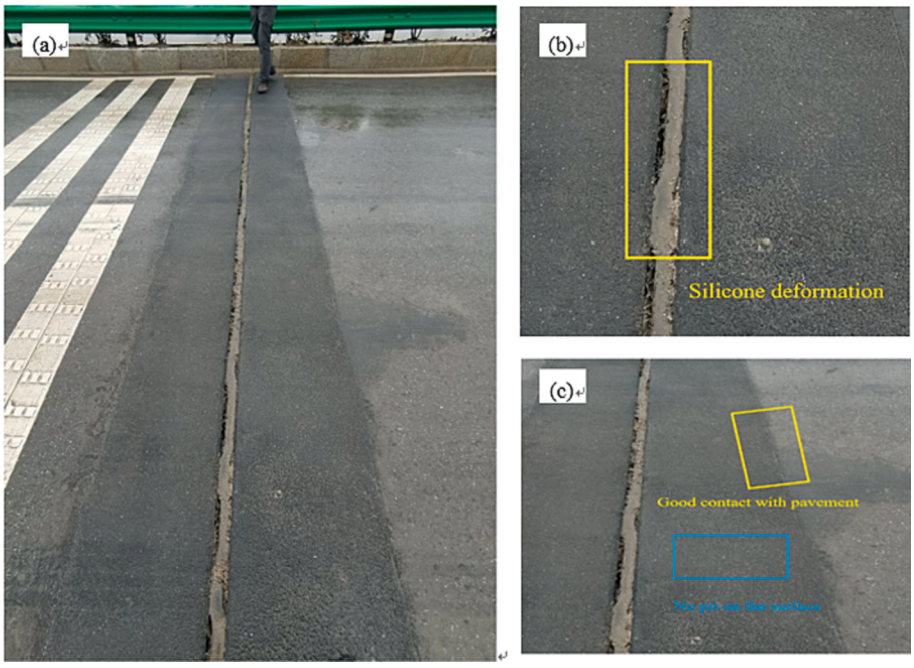

Fig. 23. SERC expansion joint.

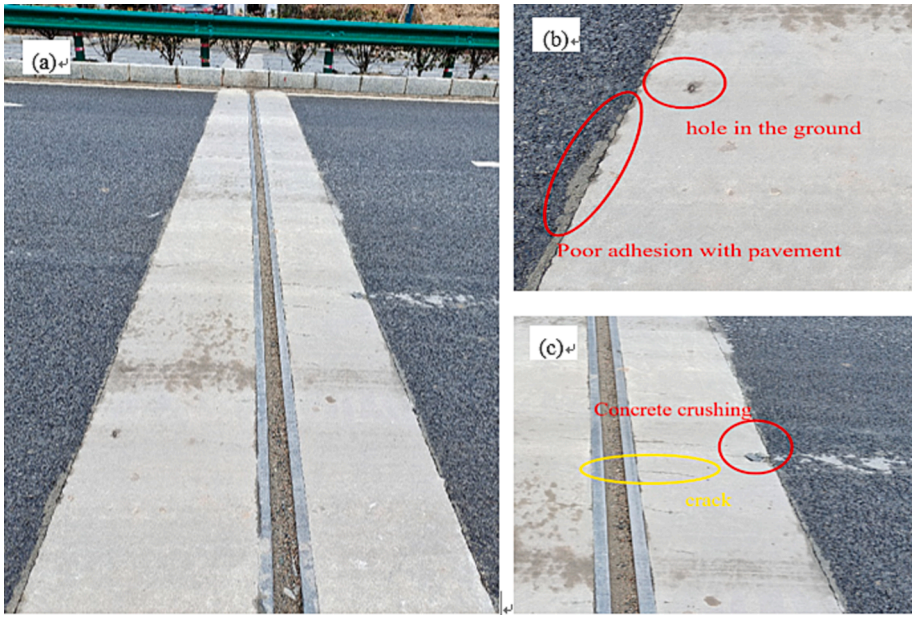

Fig. 24. UHPC concrete expansion joint.

(4) SERC and BERC have good adhesion with asphalt and high rate of strength formation, which makes it possible for SERC to be used as expansion joint and rapid repair material.
(5) Practical engineering shows that SERC as an expansion joint was completely feasible, and its performance was better than that of ordinary concrete. SERC has excellent mechanical properties, fast strength formation, high interlayer adhesion strength and good road performance. It can be used as expansion joints or pavement repair and other special parts requiring rapid opening of traffic.

Funding

The authors acknowledge the transportation technology project of department of transport of Hubei province (No. 2022-11-1-10), the scientific research fund project of Wuhan institute of technology (No. K2021032), European Union's Horizon 2020 research and innovation programme under the Marie Skłodowska-Curie grant agreement (No. 101030767), and the test help from Shiyanjia Lab (https://www.shiyanjia.com).

CRediT authorship contribution statement

Yuanyuan Li: Methodology, Data curation, Writing – original draft. **Jun Li:** Data curation, Writing – original draft, Validation. **Chao Li:** Methodology, Writing – review & editing. **Anqi Chen:** Conceptualization, Methodology, Data curation, Writing – original draft, Writing –

review & editing, Supervision, Funding acquisition. **Tao Bai:** Methodology, Project administration. **Shimin Tang:** Resources, Data curation, Software, Validation. **Shaopeng Wu:** Methodology, Data curation. **Yangming Gao:** Methodology, Validation, Funding acquisition. **Hongbin Zhu:** Data curation, Software. **Jianlin Feng:** Writing – review & editing, Data curation, Software.

Declaration of Competing Interest

The authors declare that they have no known competing financial interests or personal relationships that could have appeared to influence the work reported in this paper.

Data availability

Data will be made available on request.

References

[1] R. Li, Z. Leng, J. Yang, G.Y. Lu, M. Huang, J.T. Lan, H.L. Zhang, Y.W. Bai, Z. J. Dong, Innovative application of waste polyethylene terephthalate (PET) derived additive as an antistripping agent for asphalt mixture: experimental investigation and molecular dynamics simulation, Fuel 300 (2021).

[2] A.A.K. Sharba, A.A.G. Abu Altemen, M.M. Hason, Shear behavior of exploiting recycled brick waste and steel slag as an alternative aggregate for concrete production, Mater. Today: Proc. 42 (2021) 2621–2628.

[3] J.C.M. Ho, Y. Liang, Y.H. Wang, M.H. Lai, Z.C. Huang, D. Yang, Q.L. Zhang, Residual properties of steel slag coarse aggregate concrete after exposure to elevated temperatures, Constr. Build. Mater. 316 (2022).

[4] M.Y. Zhi, X. Yang, R. Fan, S. Yue, L.L. Zheng, Q.Y. Liu, Y.H. He, A comprehensive review of reactive flame-retardant epoxy resin: fundamentals, recent developments, and perspectives, Polym. Degrad. Stabil. 201 (2022).

[5] L. Chen, H.Y. Wang, K.R. Zheng, J. Zhou, F.Q. He, Q. Yuan, The mechanism of basic oxygen furnace steel slag retarding early-age hydration of Portland cement and mitigating approach towards higher utilization rate, J. Clean. Prod. 362 (2022).

[6] Y. Lv, S.P. Wu, P.D. Cui, Q.T. Liu, Y.Y. Li, H.Q. Xu, Y.C. Zhao, Environmental and feasible analysis of recycling steel slag as aggregate treated by silicone resin, Constr. Build. Mater. 299 (2021).

[7] Q. Dong, G.T. Wang, X.Q. Chen, J. Tan, X.Y. Gu, Recycling of steel slag aggregate in portland cement concrete: an overview, J. Clean. Prod. 282 (2021).

[8] C. Yang, S.P. Wu, P.D. Cui, S. Amirkhanian, Z.G. Zhao, F.S. Wang, L. Zhang, M. H. Wei, X.X. Zhou, J. Xie, Performance characterization and enhancement mechanism of recycled asphalt mixtures involving high RAP content and steel slag, J. Clean. Prod. 336 (2022).

[9] C.J. Shi, Z.M. Wu, K.X. Lv, L.M. Wu, A review on mixture design methods for self-compacting concrete, Constr. Build. Mater. 84 (2015) 387–398.

[10] A. Gobetti, G. Cornacchia, G. Ramorino, A. Riboldi, L.E. Depero, EAF slag as alternative filler for epoxy screeds, an example of green reuse, Sustain Mater Techno 29 (2021).

[11] Y.F. Fang, B.A. Ma, K. Wei, X.Q. Wang, X.X. Kang, F.S. Liu, Performance of single-component epoxy resin for crack repair of asphalt pavement, Constr. Build. Mater. 304 (2021).

[12] L.L. Chen, X.F. Zhang, W.Q. Ma, X.R. Zhang, Development and evaluation of a pothole patching material for steel bridge deck pavement, Constr. Build. Mater. 313 (2021).

[13] P.Z. Lu, C.H. Zhou, S.M. Huang, Y. Shen, Y.L. Pan, Experimental study on mix ratio design and road performance of medium and small deformation seamless expansion joints of bridges, Transport Res. Rec. 2675 (5) (2021) 48–59.

[14] R. Hafezzadeh, F. Autelitano, F. Giuliani, Asphalt-based cold patches for repairing road potholes – an overview, Constr. Build. Mater. 306 (2021).

[15] A. Arora, B. Singh, P. Kaur, Novel material i.e. magnesium phosphate cement (MPC) as repairing material in roads and buildings, Mater. Today: Proc. 17 (2019) 70-76.

[16] Y.Y. Li, J.L. Feng, F. Yang, S.P. Wu, Q.T. Liu, T. Bai, Z.J. Liu, C.M. Li, D.J. Gu, A. Q. Chen, Y.S. Jin, Gradient aging behaviors of asphalt aged by ultraviolet lights with various intensities, Constr. Build. Mater. 295 (2021).

[17] O. Zaid, F.M. Mukhtar, R. M-Garcia, M.G. El Sherbiny, A.M. Mohamed, Characteristics of high-performance steel fiber reinforced recycled aggregate concrete utilizing mineral filler, Case Stud. Constr. Mat. 16 (2022).

[18] M.T. Cogurcu, Investigation of mechanical properties of red pine needle fiber reinforced self-compacting ultra high performance concrete, Case Stud. Constr. Mat. 16 (2022).

[19] O. Zaid, S.R.Z. Hashmi, F. Aslam, Z. Ul Abedin, A. Ullah, Experimental study on the properties improvement of hybrid graphene oxide fiber-reinforced composite concrete, Diam. Relat. Mater. 124 (2022).

[20] Z.H. Min, Q.C. Wang, K. Zhang, L. Shen, G.F. Lin, W. Huang, Investigation on the properties of epoxy asphalt mixture containing crumb rubber for bridge expansion joint, Constr. Build. Mater. 331 (2022).

[21] M. Tabatabaeian, A. Khaloo, H. Khaloo, An innovative high performance pervious concrete with polyester and epoxy resins, Constr. Build. Mater. 228 (2019).

[22] D. Byron, A.P. Heitman, J. Neves, P.P. de Souza, P.S.D. Patricio, Evaluation of properties of polymer concrete based on epoxy resin and functionalized carbon nanotubes, Constr. Build. Mater. 309 (2021).

[23] D.M. Yu, Y.T. Fan, C. Feng, Y.C. Wu, W.D. Liu, T.F. Fu, R.H. Qiu, Preparation and performance of pervious concrete with wood tar-formaldehyde-modified epoxy resins, Constr. Build. Mater. 350 (2022).

[24] M.C. Wang, X. Tao, X.Q. Xu, R. Miao, H.Y. Du, J.C. Liu, A.R. Guo, High-temperature bonding performance of modified heat-resistant adhesive for ceramic connection, J. Alloy. Compd. 663 (2016) 82–85.

[25] A. Memar, C.M. Phan, M.O. Tade, Influence of surfactants on Fe2O3 nanostructure photoanode, Int. J. Hydrogen Energ. 37 (22) (2012) 16835–16843.

[26] G.Y. Lu, Z.J. Wang, P.F. Liu, D.W. Wang, M. Oeser, Investigation of the hydraulic properties of pervious pavement mixtures: characterization of Darcy and non-Darcy flow based on pore microstructures, J. Transp. Eng. B-Pave. 146 (2) (2020).

[27] X. Cheng, W. Tian, J. Gao, Y. Gao, Performance evaluation and lifetime prediction of steel slag coarse aggregate concrete under sulfate attack, Constr. Build. Mater. 344 (2022).

[28] L. Boquera, J.R. Castro, A.G. Fernandez, A. Navarro, A.L. Pisello, L.F. Cabeza, Thermo-mechanical stability of concrete containing steel slag as aggregate after high temperature thermal cycles, Sol. Energy 239 (2022) 59–73.

[29] S.Y. Guo, H.H. Luo, Z. Tan, J.Z. Chen, L.H. Zhang, J. Ren, Impermeability and interfacial bonding strength of TiO2-graphene modified epoxy resin coated OPC concrete, Prog. Org. Coat. 151 (2021).

[30] Y.X. Wang, Q.S. Liu, Investigation on fundamental properties and chemical characterization of water-soluble epoxy resin modified cement grout, Constr. Build. Mater. 299 (2021).

[31] Y.B. Shen, B.L. Wang, D. Li, X.R. Xu, Y.Y. Liu, Y.D. Huang, Z. Hu, Toughening shape-memory epoxy resins via sacrificial hydrogen bonds, Polym. Chem.-Uk 13 (8) (2022) 1130–1139.

[32] X. Mi, N. Liang, H. Xu, J. Wu, Y. Jiang, B. Nie, D. Zhang, Toughness and its mechanisms in epoxy resins, Prog. Mater Sci. 130 (2022).

[33] X.Q. Wang, B.A. Ma, S.S. Chen, K. Wei, X.X. Kang, Properties of epoxy-resin binders and feasibility of their application in pavement mixtures, Constr. Build. Mater. 295 (2021).

[34] Y. Xiao, M.F.C. van de Ven, A.A.A. Molenaar, S.P. Wu, Possibility of using epoxy modified bitumen to replace tar-containing binder for pavement antiskid surfaces, Constr. Build. Mater. 48 (2013) 59–66.

[35] T. Bai, Y.C. Liang, C. Li, X. Jiang, Y.Y. Li, A.Q. Chen, H. Wang, F. Xu, C. Peng, Application and validation of fly ash based geopolymer mortar as grouting material in porous asphalt concrete, Constr. Build. Mater. 332 (2022).

[36] G.Y. Lu, P.F. Liu, T. Torzs, D.W. Wang, M. Oeser, J. Grabe, Numerical analysis for the influence of saturation on the base course of permeable pavement with a novel polyurethane binder, Constr. Build. Mater. 240 (2020).

[37] A. Chen, Q. Deng, Y. Li, T. Bai, Z. Chen, J. Li, J. Feng, F. Wu, S. Wu, Q. Liu, C. Li, Harmless treatment and environmentally friendly application of waste tires—TPCB/TPO composite-modified bitumen, Constr. Build. Mater. 325 (2022).

[38] N. Bhargava, N.R. Undela, H. Nanda, A.K. Siddagangaiah, T.L. Ryntathiang, Utilizing photodetection technique to assess moisture damage of asphalt mixtures, J. Mater. Civ. Eng. 33 (11) (2021).